Dispersionless slow light in MIM waveguide based on a plasmonic analogue of electromagnetically induced transparency

Guoxi Wang, Hua Lu, and Xueming Liu*

State Key Laboratory of Transient Optics and Photonics, Xi'an Institute of Optics and Precision Mechanics, Chinese Academy of Sciences, Xi'an 710119, China

liuxueming72@yahoo.com

Abstract: We have proposed a metal-insulator-metal (MIM) waveguide system, which exhibits a significant slow-light effect, based on a plasmonic analogue of electromagnetically induced transparency (EIT). By appropriately adjusting the distance between the two stubs of a unit cell, a flat band corresponding to nearly constant group index over a broad bandwidth of 8.6 THz can be achieved. The analytical results show that the group velocity dispersion (GVD) parameter can reach zero and normalized delay-bandwidth product (NDBP) is more than 0.522. Finite-Difference Time-Domain (FDTD) simulations show that the incident pulse can be slowed down without distortion owing to the low dispersion. The proposed compact configuration can avoid the distortion of signal pulse, and thus may find potential applications in plasmonic slow-light systems, especially optical buffers.

OCIS codes: (130.3120) Integrated optics devices; (230.7370) Waveguides; (240.6680) Surface plasmons.

References and links

1. T. Baba, "Slow light in photonic crystals," Nat. Photonics **2**(8), 465–473 (2008).
2. C. Liu, Z. Dutton, C. Behroozi, and L. Hau, "Observation of coherent optical information storage in an atomic medium using halted light pulses," Nature **409**(6819), 409–411 (2001).
3. J. B. Khurgin, "Optical buffers based on slow light in electromagnetically induced transparent media and coupled resonator structures: comparative analysis," J. Opt. Soc. Am. B **22**(5), 1062–1074 (2005).
4. M. T. Hill, H. J. S. Dorren, T. De Vries, X. J. M. Leijtens, J. H. Den Besten, B. Smalbrugge, Y. S. Oei, H. Binsma, G. D. Khoe, and M. K. Smit, "A fast low-power optical memory based on coupled micro-ring lasers," Nature **432**(7014), 206–209 (2004).
5. F. Xia, L. Sekaric, and Y. Vlasov, "Ultracompact optical buffers on a silicon chip," Nat. Photonics **1**(1), 65–71 (2007).
6. M. Sandtke and L. Kuipers, "Slow guided surface plasmons at telecom frequencies," Nat. Photonics **1**(10), 573–576 (2007).
7. M. F. Yanik and S. Fan, "Stopping light all optically," Phys. Rev. Lett. **92**(8), 083901 (2004).
8. L. Yang, C. Min, and G. Veronis, "Guided subwavelength slow-light mode supported by a plasmonic waveguide system," Opt. Lett. **35**(24), 4184–4186 (2010).
9. L. Chen, G. Wang, Q. Gan, and F. J. Bartoli, "Trapping of surface-plasmon ploaritons in a graded Bragg structure: Frequency-dependent spatially separated localization of the visible spectrum modes," Phys. Rev. B **80**(16), 161106 (2009).
10. Z. Ruan and M. Qiu, "Slow electromagnetic wave guided in subwavelength region along one-dimensional perildically structured metal surface," Appl. Phys. Lett. **90**(20), 201906 (2007).
11. Q. Gan, Z. Fu, Y. J. Ding, and F. J. Bartoli, "Ultrawide-bandwidth slow-light system based on THz plasmonic graded metallic grating structures," Phys. Rev. Lett. **100**(25), 256803 (2008).
12. Q. Gan, Y. J. Ding, and F. J. Bartoli, ""Rainbow" trapping and releasing at telecommunication wavelengths," Phys. Rev. Lett. **102**(5), 056801 (2009).
13. W. L. Barnes, A. Dereux, and T. W. Ebbesen, "Surface plasmon subwavelength optics," Nature **424**(6950), 824–830 (2003).
14. D. K. Gramotnev and S. I. Bozhevolnyi, "Plasmonics beyond the diffraction limit," Nat. Photonics **4**(2), 83–91 (2010).
15. H. Lu, X. Liu, D. Mao, L. Wang, and Y. Gong, "Tunable band-pass plasmonic waveguide filters with nanodisk resonators," Opt. Express **18**(17), 17922–17927 (2010).

#170053 - $15.00 USD Received 6 Jun 2012; revised 12 Aug 2012; accepted 24 Aug 2012; published 28 Aug 2012

16. G. Wang, H. Lu, X. Liu, D. Mao, and L. Duan, "Tunable multi-channel wavelength demultiplexer based on MIM plasmonic nanodisk resonators at telecommunication regime," Opt. Express **19**(4), 3513–3518 (2011).
17. G. Wang, H. Lu, and X. Liu, "Trapping of surface plasmon waves in graded grating waveguide system," Appl. Phys. Lett. **101**(1), 013111 (2012).
18. I. De Leon and P. Berini, "Amplification of long-range surface plasmons by a dipolar gain medium," Nat. Photonics **4**(6), 382–387 (2010).
19. Z. Han, E. Forsberg, and S. He, "Surface plasmon Bragg gratings formed in metal-insulator-metal waveguides," IEEE Photon. Technol. Lett. **19**(2), 91–93 (2007).
20. H. Lu, X. Liu, D. Mao, Y. Gong, and G. Wang, "Induced transparency in nanoscale plasmonic resonator systems," Opt. Lett. **36**(16), 3233–3235 (2011).
21. H. Lu, X. Liu, and D. Mao, "Plasmonic analog of electromagnetically induced transparency in multi-nanoresonator-coupled waveguide systems," Phys. Rev. A **85**(5), 053803 (2012).
22. Y. Huang, C. Min, and G. Veronis, "Subwavelength slow-light waveguide based on a plasmonic analogue of electromagnetically induced transparency," Appl. Phys. Lett. **99**(14), 143117 (2011).
23. Q. Xu, S. Sandhu, M. L. Povinelli, J. Shakya, S. Fan, and M. Lipson, "Experimental realization of an on-chip all-optical analogue to electromagnetically induced transparency," Phys. Rev. Lett. **96**(12), 123901 (2006).
24. R. D. Kekatpure, E. S. Barnard, W. Cai, and M. L. Brongersma, "Phase-coupled plasmon-induced transparency," Phys. Rev. Lett. **104**(24), 243902 (2010).
25. J. Park, H. Kim, and B. Lee, "High order plasmonic Bragg reflection in the metal-insulator-metal waveguide Bragg grating," Opt. Express **16**(1), 413–425 (2008).
26. A. Pannipitiya, I. D. Rukhlenko, M. Premaratne, H. T. Hattori, and G. P. Agrawal, "Improved transmission model for metal-dielectric-metal plasmonic waveguides with stub structure," Opt. Express **18**(6), 6191–6204 (2010).
27. G. Veronis and S. Fan, "Bends and splitters in metal-dielectric-metal subwavelength plasmonic waveguides," Appl. Phys. Lett. **87**(13), 131102 (2005).
28. J. Liu, G. Fang, H. Zhao, Y. Zhang, and S. Liu, "Surface plasmon reflector based on serial stub structure," Opt. Express **17**(22), 20134–20139 (2009).
29. X. Piao, S. Yu, S. Koo, K. Lee, and N. Park, "Fano-type spectral asymmetry and its control for plasmonic metal-insulator-metal stub structures," Opt. Express **19**(11), 10907–10912 (2011).
30. T. Baba, T. Kawaaski, H. Sasaki, J. Adachi, and D. Mori, "Large delay-bandwidth product and tuning of slow light pulse in photonic crystal coupled waveguide," Opt. Express **16**(12), 9245–9253 (2008).
31. R. Hao, E. Cassan, H. Kurt, X. Le Roux, D. Marris-Morini, L. Vivien, H. Wu, Z. Zhou, and X. Zhang, "Novel slow light waveguide with controllable delay-bandwidth product and utra-low dispersion," Opt. Express **18**(6), 5942–5950 (2010).
32. J. Zhang, L. Cai, W. Bai, and G. Song, "Flat surface plasmon polariton bands in Bragg grating waveguide for slow light," J. Lightwave Technol. **28**(14), 2030–2036 (2010).

1. Introduction

Slow light with a remarkably low group velocity offers the possibility for time-domain processing of optical signals and enhancement of linear and nonlinear optical effects [1]. It can find important potential applications in information storage [2], optical memory [3], nonlinear optics [4] and optical buffers [5]. In general, there are three main approaches to generate slow light: quantum interference effects or EIT, photonic crystal waveguide, and stimulated Brillouin or Raman scattering [6]. So far, a variety of structures have been reported experimentally or theoretically to realize slow light [7–10]. For instance, Gan *et al*. reported a novel kind of THz plasmonic graded metallic grating structures to reduce the speed of light over an ultrawide spectral band [11], and realize "rainbow" trapping and releasing on metal surface [12]. However, previous investigations mainly focused on how to slow light on metal surface, which may bring about large scattering losses due to the poor confinement of light. In addition, utilizing the photonic bandgap (PBG) of these proposed structures, slow light can be easily observed close to the PBG bandedge. The dispersion relation around the slow light operating point inherently shows a near parabolic characteristic. This feature means that a large GVD may occur, and result in the pulse distortion, which confines the practical applications of these structures.

Surface plasmon polaritons (SPPs) have shown the ability to overcome the diffraction limit of light in microchip-sized devices, and thus are considered as one of the most promising candidates for integrated nanophotonic components [13]. In recent years, plasmonic waveguide have attracted great interests for the better confinement of light with an acceptable propagation length for SPPs [14]. Numerous devices based on plasmonic waveguide have been investigated, such as filter [15], wavelength demultiplexer [16], slow light system [17], optical amplifier [18] and Bragg reflector [19]. EIT is a quantum phenomenon that observed

#170053 - $15.00 USD Received 6 Jun 2012; revised 12 Aug 2012; accepted 24 Aug 2012; published 28 Aug 2012

in three-level atomic systems due to the quantum interference [20,21]. It features strong dispersion and slow-light propagation within the transparency window [22]. Recently, it has been demonstrated that EIT-like spectrum can be realized in classical configurations, such as coupled dielectric resonators [23] and phase-coupled plasmon-induced transparency [24].

In this paper, a plasmonic slow-light waveguide system, based on an analogue of EIT, is proposed and numerically investigated. We achieve a very flat dispersion curve with nearly constant group index over a broad frequency width of 8.6 THz. The transmission line results show that the GVD and third-order dispersion (TOD) parameters can reach zero, which means that the incident pulse can be slowed down without distortion. In addition, the NDBP of this waveguide system is calculated as high as 0.522, implying a high slow light capacity. The theoretical results are validated by the FDTD simulations. The proposed configuration can find significant applications in slow-light systems, especially optical buffers.

2. Structure model and analytical theory

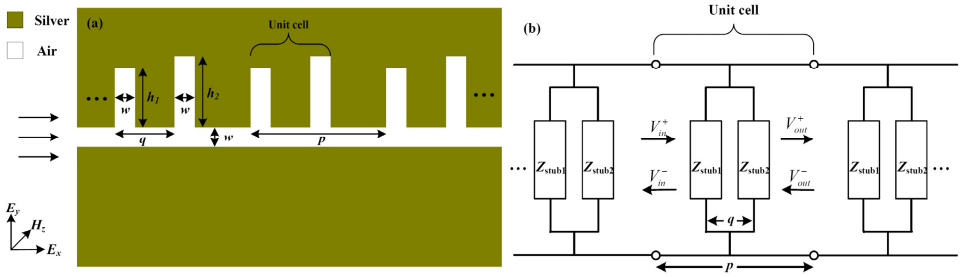

Fig. 1. (a) Schematic of the MIM plasmonic waveguide system: w, the width of the waveguide and stubs; p, the period of each unit cell; q, the distance between the two stubs in a unit cell; h, the stub depth. The light vertically illuminates the structure from the left side. (b) Equivalent circuit of the proposed plasmonic waveguide system.

Figure 1(a) shows the schematic diagram of the proposed MIM plasmonic waveguide system. When a TM-polarized plane wave is coupled into the waveguide, SPP wave can be excited at the metal-insulator interfaces and confined in the insulator layer. The metal is selected as silver, whose frequency-dependent relative permittivity is characterized by the Drude model: $\varepsilon_m(\omega) = \varepsilon_\infty - \omega_p^2/[\omega(\omega + i\gamma)]$. Here ε_∞ is the dielectric constant at infinite angular frequency, ω_p is the bulk plasma frequency and γ is the electron collision frequency. ω is the angular frequency of the incident wave in vacuum. The values of these parameters can be set as $\varepsilon_\infty = 3.7$, $\omega_p = 9.1$ eV, $\gamma = 0.018$ eV [25].

An improved transmission model [26] and transmission line theory [27] is used to account for the transmission and dispersion properties of the system. According to the transmission line theory, the plasmonic waveguide system is equivalent to a parallel connection of an infinite transmission line with the characteristic impedance of $Z_{MIM} = \beta_0 w/\omega\varepsilon_0\varepsilon_{air}$ (representing the MIM waveguide) and serial finite transmission line with the characteristic impedance Z_s terminated by a load Z_L (representing the stub). An equivalent circuit of the system is illustrated in Fig. 1(b). For simplicity, the stub section can be replaced by an effective impedance described by $Z_{stub} = Z_s(Z_L - iZ_s\tan(\beta_s h))/(Z_s - iZ_L\tan(\beta_s h))$, where $Z_s = \beta_s w/\omega\varepsilon_0\varepsilon_{air}$ and $Z_L = (\varepsilon_m/\varepsilon_{air})^{1/2} Z_s$. $\beta_0(\beta_s)$ is the propagation constant of the fundamental propagating TM mode in the MIM waveguide (stub), h is the depth of the stub. Using transmission line theory [25,28], the transmission of plasmonic waveguide system is given by $T = A((p-q)/2)B(Z_{stub1})A(p)B(Z_{stub2})A((p-q)/2)$, where the expressions of $A(x)$ and $B(stub)$ can be found in [26]. The dispersion relation between the frequency and Bolch wave number $K = \alpha + i\beta$ of the entire system can be obtained as:

#170053 - $15.00 USD Received 6 Jun 2012; revised 12 Aug 2012; accepted 24 Aug 2012; published 28 Aug 2012

$$\cos h(Kp) = \frac{1}{2}[\cos(\beta(p+q))(2+\frac{Z_{MIM}^2}{2Z_{stub1}Z_{stub2}}) - i\sin(\beta(p+q))\left(\frac{Z_{MIM}}{Z_{stub1}}+\frac{Z_{MIM}}{Z_{stub2}}\right) - \frac{1}{2}\cos(\beta(p-q))\frac{Z_{MIM}^2}{Z_{stub1}Z_{stub2}}] \quad (1)$$

3. Numerical results and discussions

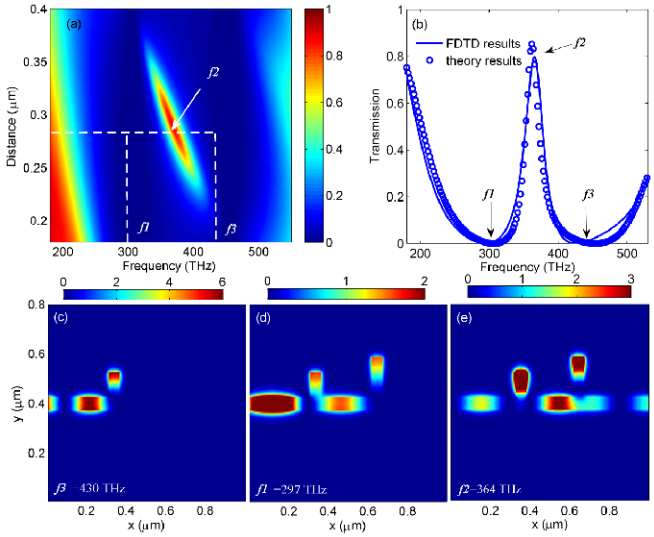

Fig. 2. (a) Evolution of transmission spectrum with the distance between the two stubs in a unit cell. The width of the waveguide and stub is w = 50 nm and the depths of the two stubs are h_1 = 100 nm and 160 nm, respectively. (b)Transmission spectrum from the transmission line theory and FDTD method for one unit cell with q = 290 nm and p = 590 nm. (c)-(e) Field distributions of $|H_z|^2$ at the transmitted-dip and induced-transparency wavelengths (Media 1, Media 2, Media 3).

一个单元

We firstly investigate the transmission properties of the MIM waveguide side-coupled to one unit cell by using the transmission line theory. The evolution of transmission spectrum with the distance q between the two stubs is shown in Fig. 2(a). When q = 290 nm, the transmission spectrum exhibits two transmitted dips and a transparency peak at 364.2 THz. The EIT-like transmission spectrum can be tuned by changing the distance between the two stubs. It should be noted that the transmission line theory cannot include the influence of the resonant mode, such as the local mode [29]. In the calculations, the propagation constant β is complex. The imaginary part of β determines the propagation length of the SPP mode, $L_{spp} = (2\mathrm{Im}\beta)^{-1}$, which is related to the metallic loss [26]. To confirm the transmission line results, the FDTD method is utilized to calculate the transmission spectrum. As shown in Fig. 2(b), there is a high-transmission peak appearing in a wide low-transmission band and the peak frequency is 364 THz with q = 290 nm, which agree well with the transmission line theory results. In Figs. 2(c)-2(d), we show the field distributions of $|H_z|^2$ at the two transmission dips (f_1 = 297 THz and f_3 = 430 THz) and the transmission peak (f_2 = 364 THz). The frequencies f_1, f_3, where the transmitted-dips occur, correspond to the resonant frequencies of the two stubs. The appearance of the transmission peak at the frequency f_2 is attributed to the destructive interference between the electromagnetic fields from the two stubs. Thus, the incident light at f_2 can propagate through the waveguide system.

#170053 - $15.00 USD Received 6 Jun 2012; revised 12 Aug 2012; accepted 24 Aug 2012; published 28 Aug 2012

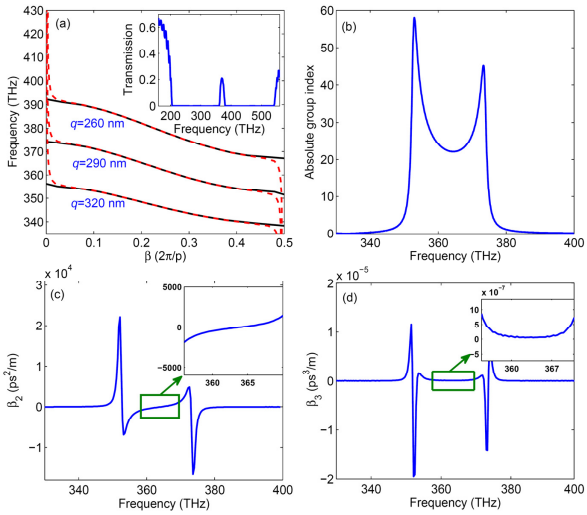

Fig. 3. (a) Dispersion curves calculated using transmission line theory (red dashed line) for different q. The parameters of the structure are: w = 50 nm, h_1 = 100 nm, h_2 = 160 nm, p = 590 nm. Inset shows the transmission for 11 unit cells with p = 700 nm. Also shown are the dispersion curves for lossless metal (black solid line). (b) Absolute group index of SPPs as a function of the frequency with q = 290 nm. (c)-(d) Second- and third-order dispersion parameters of the structure.

Successively, we study the dispersion properties of the MIM waveguide periodically coupled with unit cells. The dispersion relations for both loss and lossless metal cases with different q are shown in Fig. 3(a). In both cases, only a portion of the band structure is shown, which corresponding to the frequency range of the transparency window. One can see that when the metal loss is considered, the band structure is unchanged except at the band edges. In addition, this dispersion curve is flat and shows slightly fluctuation which indicates a nearly constant group velocity can be achieved. The inset shows the transmission for 11 unit cells, the transmission of the periodic structure is about 20%, which is higher than that in [9]. The proposed configurations may find more potential applications in plasmonic slow-light systems. From Fig. 3(b), it can be seen that the group velocity $v_g(\equiv \partial\omega/\partial\beta)$ can be slowed down in the structure. The group index of SPPs near the frequency of 364 THz shows considerable stability and nearly constant value. This indicates that slow light with zero GVD parameter can be obtained in our structure. Generally, one considers n_g to be constant within a ± 10% range, and in the sense of this criterion, we obtained a flat bandwidth over 8.6 THz, which is larger than that in [30]. The higher-order dispersions of SPP wave in the structure are also calculated. Here, the second- and third-order dispersion (TOD) parameters are characterized by $\beta_2 = d^2k/d\omega^2$ and $\beta_3 = d^3k/d\omega^3 = d\beta_2/d\omega$, respectively. As shown in Figs. 3(c) and 3(d), the GVD and TOD parameters that near the frequency of 364 THz are both equal to zero. That is to say an incident optical pulse that centered at 364 THz will suffer almost no distortion. The dispersive effect is one of the intrinsic features for the periodic structures. When appropriately tuning the geometrical parameters, the grating-induced dispersion may compensate the dispersion of the metal. Thus, a low GVD parameter can be achieved.

We also calculate the NDBP which is can be used to characterize the compromise between the light slowing down factor and the bandwidth. It is defined as NDBP$\approx\tilde{n}_g(\Delta\omega/\omega)$ [31], here $\tilde{n}_g$ denotes an average group index which is formulated as:

$$\tilde{n}_g = \int_{\omega_0}^{\omega_0+\Delta\omega} n_g(\omega)\times d\omega/\Delta\omega, \qquad (2)$$

according to the definition of the NDBP, we achieve a high NDBP value of 0.522, which is much higher than that in [31]. The high NDBP value indicates that our structure has excellent buffering capacity.

#170053 - $15.00 USD Received 6 Jun 2012; revised 12 Aug 2012; accepted 24 Aug 2012; published 28 Aug 2012

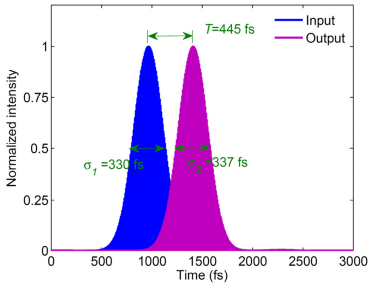

Fig. 4. Time evolution of intensity profile of the SPP pulse propagating through the waveguide system. In the FDTD simulations, 11 unit cells couple to the MIM waveguide and the other parameters are the same as that in Fig. 2(b).

To validate the above analytical results, we investigate the time evolution of the pulse propagating through the plasmonic waveguide system. The central frequency of the incident Gaussian pulse is 364 THz. The time evolution of intensity profile of the SPP pulse is shown in Fig. 4, the half-maximum at full-width of the incident pulse is 330 fs, while that of the output pulse is 337 fs. The relative pulse shape distortion is only 2.12% due to the low GVD and TOD parameters. In addition, the time for SPP pulse propagating through the waveguide system is about 445 fs. The corresponding group index $n_g' = T/T_0$ (T_0 is the propagation time of the SPP pulse through a vacuum space with the same length of the waveguide system) is 21.57, which agrees well with the transmission line reuslt (n_g = 22) shown in Fig. 3(b). Therefore, we can conclude that the incident pulse can be slowed without distortion in the plasmonic waveguide system. The coupling between the input waveguide and slow-light waveguide is also a major concern. Recently, Zhang *et al*. proposed a tapered plasmon gap waveguide to couple light into the plasmonic slow light waveguide and achieved a high coupling efficient (about 70%) [32]. This scheme can also be introduced in our waveguide to solve the coupling issue.

4. Conclusion

We propose and numerically investigate a subwavelength slow-light waveguide system. The transmission and dispersion properties are investigated by the transmission line theory. It is found that a flat dispersion curve with nearly constant group index over a broad frequency width of 8.6 THz can be obtained. It is found that the GVD and TOD parameters can reach zero, which indicates that the incident pulse can be slowed down without distortion. The NDBP of the proposed structure can reach to 0.522, implying a high slow light capacity of the proposed waveguide system. The theoretical results are validated by the FDTD simulation. This plasmonic waveguide system can find potential applications on slow-light systems.

Acknowledgments

This work was supported by the National Natural Science Foundation of China under Grants 10874239 and 10604066. The authors acknowledge helpful discussions with Dr. Jian Liang. Corresponding author (X. Liu). Tel.: + 862988881560; fax: + 862988887603; electronic mail: liuxueming72@yahoo.com and liuxm@opt.ac.cn.

#170053 - $15.00 USD Received 6 Jun 2012; revised 12 Aug 2012; accepted 24 Aug 2012; published 28 Aug 2012